Published in final edited form as:
Environ Sci Technol. 2023 April 04; 57(13): 5231–5242. doi:10.1021/acs.est.2c08806.

The Role of Mineral-Organic Interactions in PFAS Retention by AFFF Impacted Soil

Thomas Wanzek[1,*,§], **John F. Stults**[2,δ], **Mark G. Johnson**[3], **Jennifer A. Field**[4], **Markus Kleber**[1]

[1]Department of Crop and Soil Science, Oregon State University, Corvallis, Oregon 97331, United States

[2]Department Civil and Environmental Engineering, Colorado School of Mines, Golden, Colorado, 80401, United States

[3]U.S. Environmental Protection Agency, Center for Public Health and Environmental Assessment, Pacific Ecological Systems Division, Corvallis, Oregon 97333, United States

[4]Department Environmental and Molecular Toxicology, Oregon State University, Corvallis, Oregon 97331, United States

Abstract

A comprehensive, generalized approach to predict the retention of per- and polyfluoroalkyl substances (PFAS) from aqueous film forming foam (AFFF) by a soil matrix as a function of PFAS molecular and soil physiochemical properties was developed. An AFFF with 34 major PFAS (12 anions and 22 zwitterions) was added to uncontaminated soil in one-dimensional saturated column experiments and PFAS mass retained was measured. PFAS mass retention was described using an exhaustive statistical approach to generate a poly-parameter quantitative structure-property relationship (ppQSPR). The relevant predictive properties were PFAS molar mass, mass fluorine, the number of nitrogens in the PFAS molecule, poorly crystalline Fe-oxides, organic carbon, and specific (BET-N_2) surface area. The retention of anionic PFAS was nearly independent of soil properties and largely a function of molecular hydrophobicity, with the size of the fluorinated side chain as main predictor. Retention of nitrogen-containing zwitterionic PFAS was related to poorly crystalline metal oxides and organic carbon content. Knowledge of the extent to which a suite of PFAS may respond to variations in soil matrix properties, as developed here, paves the way for the development of reactive transport algorithms with the ability to capture PFAS dynamics in source zones over extended time frames.

[*]**Corresponding Author**: Phone: (541)-737-5718; Fax: (541)-737-3479; tom.wanzek@oregonstate.edu.
[§]T.W.: Geosyntec Consultants, Inc., 920 SW Sixth Avenue, Suite 600, Portland, Oregon, 97204, United States
[δ]J.F.S.: CDM Smith Inc., 14432 SE Eastgate Way Suite 100, Bellevue, Washington 98007, United States

Supporting Information
Additional details on analytical methods, sample preparation and analysis, AFFF characterization, soil characterization, soil sampling location, and column experimental set up. Tables and figures supporting the experimental and data analysis. (PDF)

Oregon State University in Corvallis, Oregon, is located within the traditional homelands of the Mary's River or Ampinefu Band of Kalapuya. Following the Willamette Valley Treaty of 1855, Kalapuya people were forcibly removed to reservations in Western Oregon. Today, living descendants of these people are a part of the Confederated Tribes of Grand Ronde Community of Oregon (grandronde.org) and the Confederated Tribes of the Siletz Indians (ctsi.nsn.us).

Graphical Abstract

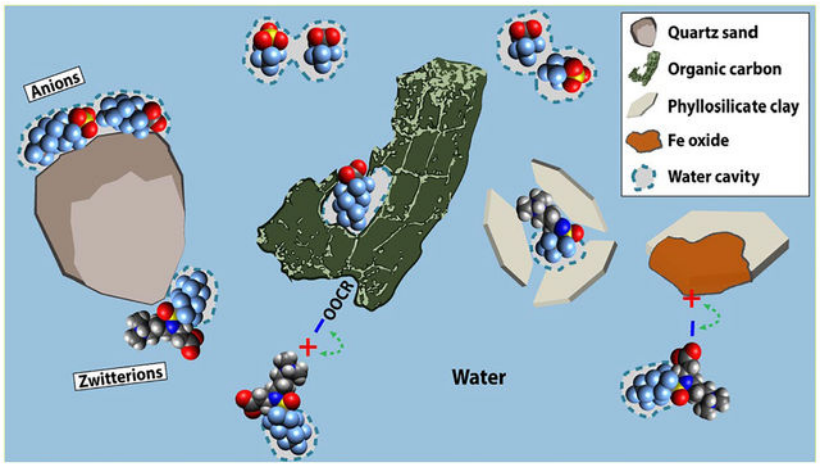

Keywords

PFAS; AFFF; soil columns; poly-parameter modeling; ppQSPR; Kd; source zone

1. INTRODUCTION

Per- and polyfluoroalkyl substances (PFAS) are an extensive family of anthropogenic compounds that are used in a variety of industrial and consumer applications, including aqueous film forming foams (AFFFs).[1–3] Soils impacted by AFFF, such as those underlying or adjacent to firefighter training areas are significant reservoirs of PFAS at both regional and global scales, even for decades after the last known AFFF application.[4–13] However, despite numerous studies that have investigated PFAS-soil interactions over the past decades,[14] a generalizable model of PFAS retention by environmental matrices has yet to emerge.[15] The challenge is to connect mechanistically relevant sorbent (i.e., soil) and sorbate (i.e., PFAS) characteristics in a way that explains retention across variable matrices at acceptable confidence levels.

Aqueous film forming foams contain multiple PFAS with various chemistries and various charge states at environmental pH range between 4 and 7. PFAS include specimens with (i) sulfonic or carboxylic acid-containing head groups bearing a single negative charge or such (ii) with a nitrogen/amine containing head group with both a positive and a negative charge (zwitterions).[16–19] The various types of PFAS commonly found in AFFF complicate the long-term management of respective AFFF impacted source zones, since molecularly different PFAS cannot be expected to exhibit similar retention characteristics when confronted with variable sorbent (i.e., soil matrix) and solvent (e.g., electrolyte concentrations in H_2O) properties (Figure 1).[20]

To date, organic carbon (OC)[21–23] and the length of the fluorinated carbon chain (as a proxy for molecular hydrophobicity) are viewed as the primary features related to PFAS partitioning to soil,[24, 25] especially for PFAS with more than six or seven fluorinated

carbons.[26–28] However, recent analyses of published soil partitioning coefficients for anionic PFAS indicate that, in soils with less than five percent OC, the fluorinated tail – OC relationship is not a robust predictor of sorption,[22, 29] with one study reporting little change in sorption with increasing OC content.[30] Several investigators also noted that the quality of the OC as opposed to the quantity alone may be a better predictor of anionic PFAS sorption.[28, 31–33] Other researchers, using column[34] and batch-based[35] experiments suggest that soil constituents and interaction mechanisms other than strict hydrophobic partitioning to OC were likely responsible for PFAS sorption. This is especially true for zwitterionic PFAS, where molecular hydrophobicity and OC are poor predictors of sorption[35] and where non-linear[26, 35, 36] or non-equilibrium[34] sorption is often observed. This view casts doubt on the validity of the current understanding that OC and number of fluorinated carbons represent the dominant controls on the retention of both anionic and zwitterionic PFAS in soil. Research of other soil properties related to sorption of anionic and zwitterionic PFAS, such as cation and anion exchange capacity,[26, 35, 37–39] pH,[21, 40] clay and sand content,[5, 38, 41–43] pore volume, and silt+clay content,[38] indicated both positive and negative correlations with varying degrees of significance for the same soil property.

It is generally possible that conflicting reports of relationships between soil and PFAS molecular properties could result from variations in experimental design. Many studies involve equilibrium batch experiments[14] while only very few employ flow-through column designs.[14, 44–51] Previous experimental designs were often focused on a limited number of primarily anionic PFAS, sourced from analytical-grade standards and thus excluding other AFFF components.[14, 26, 35, 38, 47] Media tested may not have been representative of vadose zone soils, such as pure quartz sand[44] or porous limestone.[49] The exclusion of other components common to AFFF such as hydrocarbon surfactants[52, 53] may also have confounded these experimental results, as the presence of hydrocarbon surfactants has been shown to augment PFAS retention to sediment.[54] Finally, variability in reported sorption mechanisms related to zwitterionic PFAS retention could be attributed to variations in contaminant concentration. At low (e.g., μg/L) concentrations, electrostatic soil properties were better correlated with zwitterion sorption while at higher (e.g., mg/L) concentrations hydrophobic partitioning mechanisms appeared to be more dominant.[35] In summary, most researchers conclude that no single soil or PFAS molecular property can fully capture PFAS retention in soil.[22, 26, 35, 38, 40, 55, 56]

We took this situation as a call to reconcile and improve knowledge regarding the mechanistic connection between those chemical and physical sorbent (soil) and sorbate (PFAS) properties[20, 57] that are relevant for retention and transport.[11, 15, 58]

Accordingly, our overarching goal was to develop a generalizable model of PFAS retention in saturated soils of AFFF-impacted source zones. Our conceptual approach was to simulate the initial contamination of a low OC (< 1%), low clay (< 5%) soil with PFAS by adding a commercial AFFF, diluted below its apparent critical micelle concentration, to subsurface horizons of an uncontaminated Entic Haplorthod (Rubicon Soil Series) originating from the vicinity of an existing PFAS source zone (former Wurtsmith Air Force Base, Michigan).[59, 60] Individual saturated one-dimensional (1-D) soil columns were prepared for each of the four subsurface horizons of the soil and experiments were

conducted emulating onsite hydrological conditions. To achieve the desired mechanistic connection between sorbate and sorbent properties, a statistical approach was used to generate a poly-parameter qualitative-structure property relationship (ppQSPR) between 34 PFAS and soil matrix properties. We specifically tested the assumptions that (i) soil organic carbon can serve as a single predictor value for the retention of PFAS from AFFF source zones; that (ii) soil matrix properties have potentially greater explanatory power for retention than PFAS molecular properties and that (iii) it should be possible to isolate generalizable principles to render PFAS retention fundamentally predictable.

2. MATERIALS AND METHODS

2.1. Chemicals, AFFF Characterization, and Column Effluent Analysis.

Unless noted otherwise, all chemicals and solvents were of reagent grade purchased from Fisher Scientific. For PFAS quantification, analytical standards, both native (50) and isotopically labelled (31), were purchased from Wellington Laboratories Inc. (Guelph, ON, Canada). Synthetic tap water with a total electrolyte concentration of 0.02 mM (pH ~7.2) was used to dilute the AFFF, as the aqueous phase for all experiments, and as a non-reactive tracer in this study (Table S1).

The AFFF used in the column experiments was obtained from Colorado School of Mines and previously characterized by Hao et al.[19] The PFAS we tracked through all experiments (12 anionic and 22 zwitterionic, details in Supporting Information (SI) and Table S2) were consistent with the PFAS reported in Hao et al.[19] The AFFF used in column experiments was first diluted to the proscribed 3% application strength using synthetic tap water, then further diluted (1000x)[61] until well below the apparent critical micelle concentration of 60 mg/L (Kostarelos et al.[62]). This was done to focus solely on PFAS ~ soil interactions while avoiding soil ~ micelle interactions.

PFAS in all samples were quantified using isotope dilution on a TQ Detector triple quadrupole mass spectrometer (LC-MS/MS) (Waters Corporation, Milford, MA) in both negative and positive electrospray ionization modes.[16] PFAS for which there was no matched standards were semi-quantified assuming an equal molar response to a related analyte.[16, 63] Details of the high-pressure liquid chromatography system, sample preparation procedure, mass spectrometer settings, target-surrogate combination for quantification (Table S3) and limits of detection (Table S4) can be found in the SI. Concentrations of all PFAS in the dilute AFFF and column effluent are in Tables S5 and S6, respectively.

2.2. Quality Control/Assurance for MS Analyses.

Internal continuing calibration quality control standards were analyzed every 10 samples and required to fall within 70 – 130% of the expected value. An external, third-party reference standard (Absolute Standards, Hamden, CT) containing carboxylates (C6 – 14), sulfonates (C4, 6, 8), MeFOSAA, and EtFOSAA was analyzed at the beginning of every analytical sequence and also required to fall within 70 – 130% of the expected values. The precision of the measurement of each PFAS (reported as standard deviation) during each analytical

run was measured by including at least one replicated sample (n = 4). The precision of each sample was assumed by error propagation for each PFAS from the replicated samples.

2.3. Soil Collection and Characterization.

Four PFAS-free soil horizons were collected from Oscoda-Wurtsmith Air Force base in NE Michigan (Figure S1): E, B, C1, and C2 horizons from a soil with the taxonomic class: Sandy, mixed, frigid Entic Haplorthod (Rubicon series).[64] After sampling, soil was transferred into sampling bags (4 L polyethylene bags), placed in coolers and shipped to Oregon State University. Upon receipt the soil was stored at 4 °C. Analyzed soil properties were mineral type(s) present, cation exchange capacity, organic carbon content, nitrogen content, percent sand, silt, clay, iron oxide content, specific surface area, and functional groups present on the organic carbon. Results for the analysis of soil properties are listed in Table S7.

2.4. Design of Flow-Through System and Columns.

Columns were constructed of 1 cm sections of polyvinyl chloride tubing (effective soil column length = 10 cm and inner diameter = 2.125 cm). Sections were stacked and assembled using heat-shrink tubing. Both ends were capped with mesh flow distributors and custom frit (to allow for tubing connections). Prior to packing, the soils were air dried and sieved to a particle size of ≤ 2mm. Columns for each individual soil horizon (E, B, C1, C2) were dry packed following a standardized packing procedure detailed elsewhere,[65, 66] yielding four total soil columns. Quartz sand (30/40 grade; Accusand, Ottowa, MN) was packed using the same method into n = 3 replicate columns for a total of seven columns (four soil and three Accusand colmns). The Accusand columns served as a measurement of accuracy (reported as relative standard deviation, Table S6) and as systems without any organic carbon or other soil properties with PFAS-interactive capacity (aside from surface area). The packed bulk density for E, B, C1, and C2 columns were 1.70, 1.63, 1.72, and 1.76 g cm^{-3} respectively, yielding porosities of 35, 37, 34, 32%. The average packed bulk density for the Accusand columns was 1.74 ± 0.02 g cm^{-3} (average porosity = 33%).

The packed column was connected to a flow through system which allowed for uninterrupted delivery of synthetic tap water and/or dilute AFFF (Figure S2). The system design utilized Luer tubing, valves, and fittings (Sigma Aldrich, St. Louis, MO, USA) and had an electrical conductivity electrode plumbed inline for non-reactive tracer tests. No parts containing polytetrafluoroethylene were used. To ensure that no PFAS were sorbing to the system components, after five separate test experiments, the system was flushed with methanol. No PFAS were detected in the methanol-flush effluent.

2.5. Soil Column Pack Characterization.

A non-reactive tracer experiment was conducted on each column individually prior to the start of the AFFF application experiment to calculate residence time, effective porosity, and effective pore volume. The column was oriented vertically and first saturated with ~ 10 pore volumes of deionized water (flowrate = 0.1 ml/min) in an upward flow direction to remove any entrapped air (Figure S2).[46, 62] Synthetic tap water was then applied from the top down (flow rate = 1 ml/min) and the change in electrical conductivity measured

using an inline electrical conductivity electrode and Oakton Con700 benchtop conductivity meter (Oakton Instruments, Vernon Hills, IL, USA) Once the electrical conductivity reached steady state, the column was flushed with deionized water to determine the decreasing side of the breakthrough curve. It was assumed that hydrodynamic properties of the soil packs did not change over the relatively short-duration and low flowrate experiments.[48] After the non-reactive tracer experiment and prior to the start of the AFFF experiment, each column was flushed with about five pore volumes of synthetic tap water.

2.6. Column Flow Conditions.

A mean pore water velocity of ~0.24 m/day (volumetric flowrate of ~0.064 ml/min) through the column was chosen for the AFFF experiments so as to replicate that of the natural groundwater recharge rate at Oscoda-Wurtsmith Air Force base (between 0.09 and 0.25 m/day).[67] All fluid delivery (either synthetic tap water or AFFF) was done using an Agilent 1100 HPLC pump (Agilent Technologies, Santa Clara, CA). Each column received 6.7 ml of dilute AFFF (or ~0.5 pore volumes). Following the AFFF application, synthetic tap water was flowed through the column until a minimum of ~100 ml of effluent (or six to eight pore volumes) was collected in 2 mL fractions using a Spectrum CF-2 fraction collector (Spectrum Chromatography, Houston, TX). Fractions were collected using 15 ml polypropylene tubes.

2.7. Assumptions Underlying Data Equilibrium Analysis.

The relationship between PFAS mass retained (M_R) and %OC in each soil horizon was evaluated using a model that assumed local equilibrium conditions. For each PFAS for which there was measurable breakthrough, an exact analytical solution to an advection-dispersion equation (ADE) of finite duration[68] was fit to the breakthrough curve (BTC) and used to derive a Peclet (Pe) number, a predicted injection pulse width, and a retardation factor (R_f) (Tables S8 – 11). The ADE model assumed that sorption was linear, reversible, mono-layer, and, crucially, occurring under equilibrium conditions in an advection-dominated system.[36] We evaluated the ability of the ADE model to describe PFAS sorption in or transport through the soil columns by 1) calculating an injected pulse width recovery (IPWR; acceptable range between 70% to 130%; Figure S3),[69, 70] which was calculated as the predicted pulse width divided by the applied AFFF pulse width, 2) a Pe number > 10, which indicates rapid equilibrium in an advection-dominated system,[36, 71] and 3) visual inspection of the BTCs to determine if they were generally symmetrical or characterized by early/late tailing.[72] Failure to meet any of the above assumptions and criteria can significantly decrease confidence in the resulting parameter estimations. In such instances an approach that can account for non-equilibrium or non-linear conditions will be required.[36, 71, 72]

2.8. Development of ppQSPR Model.

PFAS M_R was described using a ppQSPR linear regression analysis available in Sci-Kit learn version 1.1.2.[73] This modelling approach provided a tool to quantitatively measure the combination and relative contribution of PFAS physicochemical properties (values for all 34 PFAS are in Table S12) and soil properties (Table S7) as they related to PFAS M_R in each soil column.

First, an exhaustive or "brute-force" model optimization was conducted by fitting all possible combinations of PFAS physiochemical parameters to M_R data using linear ppQSPRs (22,802 variations in total). The linearized model calculates an intermediate mass retained value. The intermediate value was then corrected to 0% if less than 0%, or 100% if greater than 100% for the final mass retained (M_R) value. This boxcar type correction increased the sensitivity of the linearized model to changes in the intermediate range (10%−90%) without sacrificing accuracy due to bias of the highly retained (90–100% retained) or negligibly retained (0–10% retained) PFAS. We determined that a three-parameter model sufficiently described the data without over-fitting the data by comparison of the adjusted R-squared values against the number of parameters included in the model (Figure S4). Second, the selected PFAS-parameter-only model was generalized for variable soil properties by regressing the coefficients for each included parameter and the intercept against soil properties values for each horizon. The final resulting ppQSPR model (PFAS parameters + soil properties; equations 1 – 4) was selected using goodness of fit data from all four soil horizons (adjusted R-squared values and root mean squared error (RMSE)) and analysis of the metadata.[74] The final model was then externally validated against average PFAS M_R data from the three replicate Accusand columns (Figure S5). Results of the external validation test indicated that the model functioned with acceptable accuracy based on similar RMSE values to the original ppQSPR model (Table S13).

3. RESULTS AND DISCUSSION

3.1. Retention of Molecular Cohorts of PFAS as a Function of Equilibrium conditions and Soil Organic Carbon.

The power of organic carbon content as a predictor for PFAS retention was tested using two factors derived from an equilibrium-based model fitment: retardation factor (R_f) and the maximum concentration to original concentration ratio achieved (C/Co_{max}). First, all BTCs were analyzed and resulting IPWR and Pe numbers were screened to determine how well the equilibrium model fit the breakthrough data following the criteria in Methods section 2.7. In general, BTCs of anionic PFAS with seven or fewer fluorinated carbons (C) from all columns were well described by the applied equilibrium model suggesting these PFAS were in equilibrium with the soil phase. In contrast there were only a few instances where the equilibrium model was an appropriate fit to the zwitterionic PFAS BTCs (Tables S8 – 11). For $C \leq 7$ anionic PFAS, BTCs were generally symmetrical, Pe numbers were greater than 10 (though often greater than 25), and IPWR values were between 70% and 130% (Tables S8 – 11). An equilibrium model was well suited to describe retention (or breakthrough) of short-chain PFAS ($C \leq 6$) in other cases as well.[34, 75]

Example BTCs for three PFAS (Figure 2) are presented to illustrate instances where the equilibrium model was a good fit to all four BTCs (perfluorooctanoic acid; PFOA); a poor fit (perfluorooctane sulfonic acid; PFOS) or a partial fit to two of the four BTCs (N-dimethyl ammonio propyl perfluoropropane sulfonamide; AmPr-FPrSA). The BTCs for PFOA from all four soil columns were characterized by Pe numbers > 10, IPWR ranges between 70% and 130% (Table S14) and were symmetrical without any significant tailing during sorption or desorption phases (Figure 2). In contrast, PFOS breakthrough from all soil columns was

characterized by long-tailing, non-symmetrical BTCs (Figure 2), which is not well captured by a one-domain ADE.[71, 72] Similarly, IPWR values outside of the 70% to 130% range and Pe numbers < 10 were seen as potential indicators of increased dispersive transport, non-equilibrium/non-linear sorption, or effects of other non-Fickian processes which cannot be quantified by an equilibrium ADE (Tables S8 – 11).[34, 36, 72, 76]

The maximum C/Co value (C/Co_{max}) and retardation factor (R_f) derived from analysis of BTCs for PFOA and PFOS (Figure 2 and Table S14) did not correlate with the %OC in the four soil horizons. If sorption was related only to OC, we would have expected the earliest and greatest breakthrough in the soil column with the lowest %OC. The largest C/Co_{max} should have been in the C2 horizon (lowest %OC = 0.02%) with the lowest C/Co_{max} in the B horizon (%OC = 0.28%) (Figure 2). Instead PFOA in the E and C2 columns had similar C/Co_{max} values (0.83 and 0.86 respectively) and the B and C1 columns reached similar C/Co_{max} values (0.64 and 0.65 respectively). In terms of R_f, the highest value would have been expected in the column with the most %OC if that was the main phase with which PFAS were interacting. PFOA broke through earliest in the E horizon column (R_f = 0.9) while the B, C1, and C2 columns had similar R_fs (1.2, 1.3, and 1.2 respectively). Retardation factors for PFOS showed a similar lack of correlation with %OC, with similar R_fs in the B and C2 columns (5.0 and 4.8 respectively) and the E and C1 columns (3.1 and 2.8 respectively). All retardation factors which could be calculated are in Tables S8 – 11.

There was a similar trend in the PFOS BTCs to that of PFOA in that there was no correlation with %OC. The E and C1 columns had similar R_fs (3.1 and 2.8 respectively; Table S14) and C/Co_{max} values (0.16 and 0.17 respectively) and the C2 horizon was more retarded (R_f = 4.5) and had a lower C/Co_{max} (0.11). The B horizon had the most retarded breakthrough (R_f = 5.0) and lowest C/Co_{max} (0.08). It should be noted that none of the PFOS BTCs met the criteria set for analysis using the equilibrium ADE (Table S14), and thus R_f values are likely underestimated. The lack of correlation between %OC and PFAS interaction with soil (as described by the soil partitioning coefficient, K_d) was also described in a meta-analysis of published K_d ~ %OC data by Li et al.[22] They concluded that, once removing sorption data derived from high OC soil, the relationship between K_d and OC content became weaker or altogether insignificant.

Breakthrough of the three-carbon zwitterion AmPr-FPrSA from two of the columns, C1 and C2, could be fit by the equilibrium model but not those from the E and B columns (Table S14). In contrast to PFOA and PFOS, AmPr-FPrSA interaction with the soil horizons did correlate with %OC. The C2 column had the smallest R_f (1.5) and highest C/Co_{max} value (0.54), followed by the C1 column (R_f = 1.8 and C/Co_{max} = 0.42), the E column (R_f = 5.3 and 0.09), and finally the B column (R_f = 16.4 and C/Co_{max} = 0.08). Though R_f values are listed for AmPr-FPrSA in the E and B columns, they are likely underestimated as they violated the criteria set for equilibrium analysis and exhibited what appears to be non-linear or hysteretic sorption behavior, which has been observed by others.[34, 35] For PFAS where the equilibrium model could not be used (e.g., the majority of the zwitterionic PFAS) it is likely that sorption processes/mechanisms such as electrostatic interactions, as opposed to a hydrophobic exclusion mechanism, were active.[34–36]

We then examined the dataset as a whole for commonalities in retention behavior of all 34 PFAS from all four soil columns based on the observations from the comparison of the three example PFAS. Retention of all PFAS was found to loosely sort into two large molecular cohorts (Figure 3). Across the four soil horizons examined, M_R was between 0 and ~15% for C3 to C5 anionic PFAS and generally below 30% for all anionic PFAS with less than eight fluorinated carbons. Complete retention (M_R = 100%) was a rare exception, even for those that had eight fluorinated carbons (Figure 3). Overall, the retention of anionic C ≤ 7 PFAS did not correlate with the OC content in any of the four soil columns (Figure 3), indicating that, in low OC systems at least, OC content is not predictive for PFAS retention.[22, 28–30, 32]

In the case of zwitterionic PFAS, complete retention (M_R = 100%) was the norm (Figure 3) with a minority of zwitterionic PFAS breaking through (M_R < 100%) after five pore volumes of water. The spread in M_R was greatest for C ≤ 4 zwitterionic PFAS. Zwitterions with five or more fluorinated carbons had at least 50% of their mass retained, even in the soil columns with the lowest percent OC (0.02% OC). No mass for C6 and C7 zwitterions broke through any of the soil columns (M_R = 100%).

Similarly in the Accusand columns, which were free of organic carbon, PFAS mass was retained. Mass was retained as a function of PFAS type and, in the case of the zwitterions, as a function of the number of fluorinated carbons (Figure 4). Similar to the soil columns, M_R increased with increasing number of fluorinated carbons. Retention of C4 and shorter zwitterions was ~20% with retention increasing with the number of fluorinatead carbons. Retention of anionic PFAS did not increase as a function of the number of fluorinated carbons, but instead all M_R values were between ~10% to ~20%. It is likely that both cohorts of PFAS molecules were being hydrophobically excluded and partitioning to the aqueous-solid interface as a way to escape the aqueous phase. Interestingly, the variability in the M_R data was greater for anions than for zwitterions (error bars in Figure 4). This suggests that retention of anionic PFAS may be more a function of media transport properties[36, 77] and pore network geometries (which were not measured as a part of this research) and less dependent on surface interactions.

Our data indicate that the OC concentration in the soil matrix was not a robust predictor for the retention of anionic PFAS and clearly not the only predictor for the retention of zwitterionic PFAS. Sorption of PFAS in systems devoid of organic carbon has also been observed by others.[48] Shafique et al.[78] found that hydrophobic exclusion was strong enough to aggregate anionic PFAS on apolar siloxane patches on the surface of silica grains. They also found that physical reorientation of the molecule was sufficient to overcome any electrostatic repulsion encountered by the head group and surface silanol groups. Similarly, on a surface-area normalized basis, silica sand had the highest sorptive capacity for PFOS compared to goethite, kaolinite, or iron-enriched sand.[55] Others have also observed preferential sorption of PFAS to silaceous zeolite compounds in the absence of OC.[79, 80] Accordingly, we reject the assumption that organic carbon content can be used as a single predictor variable for PFAS M_R (assumption one).

3.2. Model Results and Validation.

With the absence of an obvious single value predictor for PFAS retention, the development of a more comprehensive model was indicated. Physiochemical - soil property relationships were established for a total of 136 PFAS-sorbent combinations (34 PFAS × 4 soil horizons) and assessed for their ability to describe the total capacity of a soil to retain a given PFAS molecule. This resulted in the down selection of n = 14 PFAS physiochemical and n = 9 soil predictor variables (Tables S12 and S7 respectively) and eventually yielded the following model:

$$X = \{[0.204 * PFAS\ molar\ mass] + [0.318 * mass\ fluorine] + [c * nitrogens] + Z] \pm 16.2 \quad (1)$$

$$c = \{[3.5 * FeOx] + [89.7 * \%\ OC] + 22.7\} \quad (2)$$

$$Z = \{[0.12 * SA_{BET}] - 146\} \quad (3)$$

$$M_R = \begin{cases} 100 & if \quad X > 100 \\ X & if \quad 100 \geq X \geq 0 \\ 0 & if \quad X < 0 \end{cases} \quad (4)$$

where X is the intermediate percent mass retained estimate, which is a function of *PFAS molar mass* (the mass of the PFAS molecule), *mass fluorine* (total mass of fluorine on the PFAS molecule calculated as the number of fluorine atoms on the PFAS molecule times the molar mass of fluorine; 19 g/mol), *nitrogens* (the number of nitrogen atoms in the PFAS molecule) (Eq. 1), Fe_{Ox} (the amount of oxalate extractable iron (g Fe kg^{-1} soil)), *%OC* (mass percentage of organic carbon in the soil) (Eq. 2), and SA_{BET} (specific surface area of the soil ($m^2\ g^{-1}$)) (Eq. 3) ($r^2 = 0.84$, $p < 0.001$). M_R (Eq. 4) is the final percent mass retained of a given PFAS molecule in the soil of interest. To determine the overall model accuracy, the RMSE was calculated and determined to be ± 16.2%.[74] Among the down-selected predictor variables (Table S15), the parameters *PFAS molar mass* and *number of nitrogens* (individual r^2 values of 0.51 and 0.5, respectively) dominated, but carried insufficient individual power to enable satisfactory predictions. Accordingly, consideration of the parameters: *mass fluorine*, *OC*, Fe_{ox} and SA_{BET} was necessary to maximize the predictive power of the model. The relative contribution of each model parameter can be quantified as a function of each parameter's coefficient (analysis and ranges of parameter values are in Figure S6 and Table S15 respectively). The *molar mass* and *mass fluorine* have similar impacts on overall M_R (coefficients = 0.204 and 0.318 respectively) where the *nitrogen* parameter is more heavily weighted due to the statistical relationship to two soil parameters (Fe_{Ox} and *%OC*; coefficients = 3.5 and 89.7 respectively). From a mechanistic perspective, including SA_{BET} was important as all PFAS need a surface to interact with, but the parameter had negligible impact on the overall performance of the model (coefficient = 0.12; only changed M_R by ~1%). With this data we partially accept assumption two. A combination of soil properties and PFAS molecular properties are influential in sorption

of zwitterionic PFAS while mainly molecular properties are related to sorption of anionic PFAS.

3.3. Model predictions.

Satisfactory model performance was demonstrated by plotting experimentally measured M_R as a function of model predicted M_R for each of the four soil horizons (Figure 5).

The fact that soil horizon data do not cluster in certain locations of the plot validates the choice of predictor variables and confirms the general applicability of the model. Similar plots were constructed using PFAS molar mass and number of nitrogens as predictor variables; Figures S7 and S8), illustrating the individual weight of these variables. Doing so confirmed two basic tenets of PFAS retention: M_R increases with PFAS molar mass,[81] and with the frequency of N-containing groups.[34, 82] The latter observation can be further emphasized by examining two PFAS that have similar molar mass, but differ in nitrogen content: perfluoroheptane sulfonic acid (PFHpS) (no nitrogen, molar mass = 450 g/mol) showed an average M_R across the four different soil matrices of 12.4%, while N-sulfo propyl dimethyl ammonio propyl perfluoropropane sulfonamide (SPrAmPr-FPrSA) (two nitrogens, molar mass = 456 g/mol) had an average M_R of 57.5%, almost four times as high. Here we confirm assumption three that PFAS retention follows generalizable principles.

3.4. Model Validation.

The model was subjected to an external validation test using PFAS M_R data from the replicate (n = 3) Accusand columns. Model performance was assessed through the parameters root mean squared error (RMSE) and coefficient of determination (r^2) and found to be satisfactory (Table S13; Figure S5). Similar RMSE values from internal model calibration (16.2) and external model validation (16.3, $r^2 = 0.78$) indicate good model performance[74] in terms of predicting PFAS M_R.

In a a second external validation exercise, we took advantage of a recent study by Adamson et al.[4] who used a comprehensive hydrological modeling approach to assess the mass of PFOS retained by the soil underlying the fire training area at a naval air station. Adamson et al.[4] calculated that after decades of exposure to AFFF, the soil in that fire training area still contained ~40 kg of PFOS. Using publicly available soil data (https://websoilsurvey.nrcs.usda.gov) specific to that site and the necessary molecular properties of PFOS, our ppQSPR model independently predicted that the same soil would be able to retain a total of 47.8 kg of PFOS, which is in good agreement with the estimate by Adamson et al.[4]

3.5. Mechanistic considerations and plausibility of underlying assumptions.

Exclusion of PFAS molecules *from* the aqueous phase may be an important step in the retention of both anions and zwitterions on soil surfaces. Two of the three PFAS physiochemical properties included in the ppQSPR model, *PFAS molar mass* and *mass fluorine*, capture the likelihood of a given molecule to be excluded from the aqueous phase. This insight is complementary to free energy calculations carried out by Xiao et al.,[35] who found that exclusion of both cations and zwitterions *from* the aqueous phase

was one of the predominant driving forces for adsorption to soil surfaces. As the *molar mass* of the PFAS increases, the thermodynamic 'force' or motivation for the molecule to be expelled from the aqueous phase also increases.[24, 83] The step of exclusion from the aqueous phase likely applies to anions as well since Xiao et al.[35] found that both anionic and zwitterionic PFAS of the same perfluorinated carbon chain length had similar degrees of hydrophobicity. However, it is important to note the absence of any correlation between strictly anionic PFAS and Fe_{ox} and *%OC*, suggesting that anions do not interact electrostatically with sorbent surfaces. Instead, anions are likely excluded from the aqueous phase to any available surface or interface as a function of their relative hydrophobicity. Others such as Xiao et al.[35] reported that the electrostatic potential of zwitterions was several orders of magnitude higher than that of anions, leaving anions with a reduced capacity to interact electrostatically. Using a batch study, Nguyen et al.[38] found that anion sorption was best described by a combination of %OC, silt+clay content, and micropore volume, two of which describe the amount of potential interaction space or surfaces in the soil. This is in agreement with our interpretation that anions likely have a similar affinity for any available solid interface.[41]

Our modeling activity led to the finding that sorbent parameters Fe_{ox} and *%OC* were statistically related to the *number of nitrogens* parameter, meaning that they influence the retention of zwitterionic PFAS that possess both positive and negative charges, thus underlining the plausibility of a mechanistic contribution of these structural PFAS features to interactions with charged soil surfaces.[26, 34, 37] This is noteworthy as Al/Fe oxides contribute positive charge at typical soil pH ranges, while well decomposed organic carbon carries net negative charge and can serve as a potent cation exchange medium.[84, 85] Several considerations may help to constrain the underlying mechanisms of zwitterionic sorption. First, charges on zwitterionic PFAS may be more shielded from the electron-withdrawing fluorinated tail by other interspaced atoms (Table S2). This may allow for the charge(s) on their head groups to be stronger and less delocalized compared to the negative charge on anionic PFAS, thus increasing their capacity to interact with charged soil components. This hypothesis is supported by Parker et al.[86] who observed that anionic PFAS with $–CH_2–$ spacers between the fluorinated tail and the charged head group (e.g., a *poly*fluorinated fluorotelomer sulfonate) had an overall more negative electrostatic charge than those without the $–CH_2–$ spacer. A second possibility is that the non-fluorinated aliphatic head groups which, in contrast to the highly lipophobic fluorocarbon chain, should impart some capacity to engage in Van der Waals type interactions with hydrophobic soil components. A third option is that PFAS with a negatively charged propanoic acid head group, for example N-dimethyl ammonio propyl perfluorohexane sulfonamido propanoic acid (AmPr-FHxSA-PrA) may orient itself toward the positively charged terminal amine group (Figure S9), creating a net charge on the molecule that is likely close to zero. The geometrically optimized structure of AmPr-FHxSA-PrA (optimized with the Merck molecular force field (MMFF94)[87] in Avogadro,[88] as previously performed for PFAS[89, 90]) supports this hypothesis with the propanoic acid contorted toward the terminal amine. In contrast, the geometrically optimized structure of N-dimethyl ammonio propyl perfluorohexane sulfonamide (AmPr-FHxSA; Figure S10), which does not have a propanoic acid in its head group, was largely linear. The coordinates of the geometrically optimized AmPr-FHxSA-

PrA and AmPr-FHxSA are provided in the SI (Tables S16 and S17). The computational predictions may explain why some zwitterionic PFAS may behave as 'neutral' molecules with zero net charge[20] and why zwitterion mass retained was related to the largely aliphatic OC in this soil; whereas no such relationship was found for anionic C ≤ 7 PFAS.

When generating the ppQSPR model we assumed the included parameters behaved independent of concentration (i.e., followed a linear isotherm) with a Freundlich non-linearity term (n) equal to 1 (an n-value of 1 indicates isotherm linearity). Though we did not directly calculate n, the presence or absence of sorption non-linearity of PFAS in soils has been previously investigated by others using soil similar to those used in our experiments.[14, 91] Specifically, Van Glubt et al.,[14] used the Freundlich isotherm model to examine the non-linearity of PFOS and PFOA adsorption to sandy soils using batch and column experiments. Results of their analysis generated a n value that was near 1 (0.7–0.9),[14] indicating that isotherm non-linearity was mild to moderate at most. One of the primary drivers of isotherm non-linearity consistent with Freundlich behavior is known to be the energetic heterogeneity of surface adsorption sites.[92] Because our soil was highly sandy and relatively homogeneous, similar to the soil used by Van Glubt et al.,[14] sorption non-linearity likely did not influence PFAS retention in a significant way.

Inversions of HYDRUS equilibrium and two site non-equilibrium models were conducted for three example PFAS (PFBA, PFOS, AmPr-FPrSA; 12 total PFAS/soil simulations) to briefly examine if retention was influenced by rate-limited adsorption. Equilibrium models were more appropriate in 11 of the 12 simulations and non-equilibrium effects were mild to negligible in the one scenario for which the non-equilibrium model was more appropriate (Table S18). These results indicate that PFAS retention was not significantly influenced by rate-limited adsorption. The HYDRUS model results are also consistent with the significant mass retention we observed for most of the zwitterionic and long chain anions as well as results from Geulfo et al.,[48] who found predominantly equilibrium behavior in low OC soils at similar experimental flow rates.

4. IMPLICATIONS

Several generalizable insights were generated by our investigation. The soil used in our experiments had matrix properties similar to those of soils underlying at least another 15 military source zones across the US, rendering the insights obtained broadly applicable. With regard to the relevance of PFAS molecular properties, it became apparent that it is necessary to distinguish between zwitterions and anionic PFAS when considering the propensity for retention in a soil. Among the latter group, retention is generally low until the fluorinated chain comprises at least eight (8) fluorinated carbon atoms. Even more important for site managers and policy makers is the observation that for anionic PFAS, surface properties of systems with negligible organic carbon content cannot predict PFAS retention. For anionic PFAS compounds, the overriding control on sorption to soil is the size of the fluorinated carbon chain and the associated thermodynamic 'force' or motivation to be expelled from the aqueous phase.

The situation is different for zwitterionic PFAS. For the zwitterions present in our AFFF formulation, PFAS molar mass and the number of N atoms incorporated were the dominant molecular controls, but these substances also showed significant tendencies to actually interact with charged portions of the soil matrix. Given the fact that the soil chosen for this investigation was coarse textured with limited surface reactivity, and hence a very poor sorbent, we feel justified to deduce that any soil matrix with finer texture and greater surface reactivity will retain both anionic and zwitterionic PFAS to a significantly larger extent.

Finally, our research showed that the fraction of soil organic carbon present (f_{OC}) does not represent a single value predictor for retention of all PFAS in source zones[26, 32, 38, 93] and that variables such as the surface reactivity of the mineral phase[55, 94] or the quality of the organic carbon need to be considered as well.[28, 33] This observation is particularly relevant given the widespread practice to derive retention characteristics from K_d values estimated from the fraction of organic matter.

Supplementary Material

Refer to Web version on PubMed Central for supplementary material.

ACKNOWLEDGEMENTS

The study was supported by the Strategic Environmental Research and Defense Program Grant ER-1259. The authors would also like to thank Dr. Ivan A. Titaley (Oregon State University, Department of Environmental and Molecular Toxicology) for his help with computational optimization of PFAS structures and electrostatic potential modelling and Adam Lindsley (Oregon State University, Teaching & Engagement Department) for the ToC art design. The authors also appreciate the three anonymous reviewers for giving their time and effort to improve the content and overall quality of this manuscript.

REFERENCES

(1). Buck RC; Franklin J; Berger U; Conder JM; Cousins IT; de Voogt P; Jensen AA; Kannan K; Mabury SA; van Leeuwen SP Perfluoroalkyl and polyfluoroalkyl substances in the environment: terminology, classification, and origins. Integr Environ Assess Manag 2011, 7 (4), 513–541. DOI: 10.1002/ieam.258. [PubMed: 21793199]

(2). Gluge J; Scheringer M; Cousins IT; DeWitt JC; Goldenman G; Herzke D; Lohmann R; Ng CA; Trier X; Wang Z An overview of the uses of per- and polyfluoroalkyl substances (PFAS). Environ Sci Process Impacts 2020, 22 (12), 2345–2373. DOI: 10.1039/d0em00291g. [PubMed: 33125022]

(3). Prevedouros K; Cousins IT; Buck RC; Korzeniowski SH Sources, fate and transport of perfluorocarboxylates. Environ Sci Technol 2006, 40 (1), 32–44. DOI: 10.1021/es0512475. [PubMed: 16433330]

(4). Adamson DT; Nickerson A; Kulkarni PR; Higgins CP; Popovic J; Field J; Rodowa A; Newell C; DeBlanc P; Kornuc JJ Mass-Based, Field-Scale Demonstration of PFAS Retention within AFFF-Associated Source Areas. Environ Sci Technol 2020, 54 (24), 15768–15777. DOI: 10.1021/acs.est.0c04472. [PubMed: 33270425]

(5). Hunter Anderson R; Adamson DT; Stroo HF Partitioning of poly- and perfluoroalkyl substances from soil to groundwater within aqueous film-forming foam source zones. J Contam Hydrol 2019, 220, 59–65. DOI: 10.1016/j.jconhyd.2018.11.011. [PubMed: 30527585]

(6). Anderson RH; Long GC; Porter RC; Anderson JK Occurrence of select perfluoroalkyl substances at U.S. Air Force aqueous film-forming foam release sites other than fire-training areas: Field-validation of critical fate and transport properties. Chemosphere 2016, 150, 678–685. DOI: 10.1016/j.chemosphere.2016.01.014. [PubMed: 26786021]

(7). Bekele DN; Liu Y; Donaghey M; Umeh A; Arachchige CSV; Chadalavada S; Naidu R Separation and Lithological Mapping of PFAS Mixtures in the Vadose Zone at a Contaminated Site. Frontiers in Water 2020, 2. DOI: 10.3389/frwa.2020.597810.

(8). Brusseau ML; Anderson RH; Guo B PFAS concentrations in soils: Background levels versus contaminated sites. Sci Total Environ 2020, 740, 140017. DOI: 10.1016/j.scitotenv.2020.140017. [PubMed: 32927568]

(9). Houtz EF; Higgins CP; Field JA; Sedlak DL Persistence of perfluoroalkyl acid precursors in AFFF-impacted groundwater and soil. Environ Sci Technol 2013, 47 (15), 8187–8195. DOI: 10.1021/es4018877. [PubMed: 23886337]

(10). Hu XC; Andrews DQ; Lindstrom AB; Bruton TA; Schaider LA; Grandjean P; Lohmann R; Carignan CC; Blum A; Balan SA; Higgins CP; Sunderland EM Detection of Poly- and Perfluoroalkyl Substances (PFASs) in U.S. Drinking Water Linked to Industrial Sites, Military Fire Training Areas, and Wastewater Treatment Plants. Environ Sci Technol Lett 2016, 3 (10), 344–350. DOI: 10.1021/acs.estlett.6b00260. [PubMed: 27752509]

(11). Maizel AC; Shea S; Nickerson A; Schaefer C; Higgins CP Release of Per- and Polyfluoroalkyl Substances from Aqueous Film-Forming Foam Impacted Soils. Environ Sci Technol 2021, 55 (21), 14617–14627. DOI: 10.1021/acs.est.1c02871. [PubMed: 34665614]

(12). Newell CJ; Adamson DT; Kulkarni PR; Nzeribe BN; Connor JA; Popovic J; Stroo HF Monitored Natural Attenuation to Manage PFAS Impacts to Groundwater: Scientific Basis. Groundwater Monitoring & Remediation 2021, 41 (4), 76–89. DOI: 10.1111/gwmr.12486.

(13). Rankin K; Mabury SA; Jenkins TM; Washington JW A North American and global survey of perfluoroalkyl substances in surface soils: Distribution patterns and mode of occurrence. Chemosphere 2016, 161, 333–341. DOI: 10.1016/j.chemosphere.2016.06.109. [PubMed: 27441993]

(14). Van Glubt S; Brusseau ML; Yan N; Huang D; Khan N; Carroll KC Column versus batch methods for measuring PFOS and PFOA sorption to geomedia. Environ Pollut 2021, 268 (Pt B), 115917. DOI: 10.1016/j.envpol.2020.115917. [PubMed: 33143983]

(15). Guelfo JL; Korzeniowski S; Mills MA; Anderson J; Anderson RH; Arblaster JA; Conder JM; Cousins IT; Dasu K; Henry BJ; Lee LS; Liu J; McKenzie ER; Willey J Environmental Sources, Chemistry, Fate, and Transport of Per- and Polyfluoroalkyl Substances: State of the Science, Key Knowledge Gaps, and Recommendations Presented at the August 2019 SETAC Focus Topic Meeting. Environ Toxicol Chem 2021, 40 (12), 3234–3260. DOI: 10.1002/etc.5182. [PubMed: 34325493]

(16). Backe WJ; Day TC; Field JA Zwitterionic, cationic, and anionic fluorinated chemicals in aqueous film forming foam formulations and groundwater from U.S. military bases by nonaqueous large-volume injection HPLC-MS/MS. Environ Sci Technol 2013, 47 (10), 5226–5234. DOI: 10.1021/es3034999. [PubMed: 23590254]

(17). Barzen-Hanson KA; Field JA Discovery and Implications of C2 and C3 Perfluoroalkyl Sulfonates in Aqueous Film-Forming Foams and Groundwater. Environmental Science & Technology Letters 2015, 2 (4), 95–99. DOI: 10.1021/acs.estlett.5b00049.

(18). Barzen-Hanson KA; Roberts SC; Choyke S; Oetjen K; McAlees A; Riddell N; McCrindle R; Ferguson PL; Higgins CP; Field JA Discovery of 40 Classes of Per- and Polyfluoroalkyl Substances in Historical Aqueous Film-Forming Foams (AFFFs) and AFFF-Impacted Groundwater. Environ Sci Technol 2017, 51 (4), 2047–2057. DOI: 10.1021/acs.est.6b05843. [PubMed: 28098989]

(19). Hao S; Choi YJ; Wu B; Higgins CP; Deeb R; Strathmann TJ Hydrothermal Alkaline Treatment for Destruction of Per- and Polyfluoroalkyl Substances in Aqueous Film-Forming Foam. Environ Sci Technol 2021, 55 (5), 3283–3295. DOI: 10.1021/acs.est.0c06906. [PubMed: 33557522]

(20). Lyu X; Xiao F; Shen C; Chen J; Park CM; Sun Y; Flury M; Wang D Per- and Polyfluoroalkyl Substances (PFAS) in Subsurface Environments: Occurrence, Fate, Transport, and Research Prospect. Reviews of Geophysics 2022, 60 (3). DOI: 10.1029/2021rg000765.

(21). Higgins CP; Luthy RG Sorption of perfluorinated surfactants on sediments. Environ Sci Technol 2006, 40 (23), 7251–7256. DOI: 10.1021/es061000n. [PubMed: 17180974]

(22). Li Y; Oliver DP; Kookana RS A critical analysis of published data to discern the role of soil and sediment properties in determining sorption of per and polyfluoroalkyl substances (PFASs). Sci Total Environ 2018, 628–629, 110–120. DOI: 10.1016/j.scitotenv.2018.01.167.

(23). Sigmund G; Arp HPH; Aumeier BM; Bucheli TD; Chefetz B; Chen W; Droge STJ; Endo S; Escher BI; Hale SE; Hofmann T; Pignatello J; Reemtsma T; Schmidt TC; Schonsee CD; Scheringer M Sorption and Mobility of Charged Organic Compounds: How to Confront and Overcome Limitations in Their Assessment. Environ Sci Technol 2022, 56 (8), 4702–4710. DOI: 10.1021/acs.est.2c00570. [PubMed: 35353522]

(24). Goss KU; Bronner G What is so special about the sorption behavior of highly fluorinated compounds? J Phys Chem A 2006, 110 (30), 9518–9522. DOI: 10.1021/jp062684o. [PubMed: 16869704]

(25). Krafft MP; Riess JG Selected physicochemical aspects of poly- and perfluoroalkylated substances relevant to performance, environment and sustainability-part one. Chemosphere 2015, 129, 4–19. DOI: 10.1016/j.chemosphere.2014.08.039. [PubMed: 25245564]

(26). Barzen-Hanson KA; Davis SE; Kleber M; Field JA Sorption of Fluorotelomer Sulfonates, Fluorotelomer Sulfonamido Betaines, and a Fluorotelomer Sulfonamido Amine in National Foam Aqueous Film-Forming Foam to Soil. Environ Sci Technol 2017, 51 (21), 12394–12404. DOI: 10.1021/acs.est.7b03452. [PubMed: 28968065]

(27). Guelfo JL; Higgins CP Subsurface transport potential of perfluoroalkyl acids at aqueous film-forming foam (AFFF)-impacted sites. Environ Sci Technol 2013, 47 (9), 4164–4171. DOI: 10.1021/es3048043. [PubMed: 23566120]

(28). Li F; Fang X; Zhou Z; Liao X; Zou J; Yuan B; Sun W Adsorption of perfluorinated acids onto soils: Kinetics, isotherms, and influences of soil properties. Sci Total Environ 2019, 649, 504–514. DOI: 10.1016/j.scitotenv.2018.08.209. [PubMed: 30176462]

(29). Rovero M; Cutt D; Griffiths R; Filipowicz U; Mishkin K; White B; Goodrow S; Wilkin RT Limitations of Current Approaches for Predicting Groundwater Vulnerability from PFAS Contamination in the Vadose Zone. Ground Water Monit Remediat 2021, 41 (4), 62–75. DOI: 10.1111/gwmr.12485. [PubMed: 35087263]

(30). Pan G; You C Sediment-water distribution of perfluorooctane sulfonate (PFOS) in Yangtze River Estuary. Environ Pollut 2010, 158 (5), 1363–1367. DOI: 10.1016/j.envpol.2010.01.011. [PubMed: 20170997]

(31). Longstaffe JG; Courtier-Murias D; Soong R; Simpson MJ; Maas WE; Fey M; Hutchins H; Krishnamurthy S; Struppe J; Alaee M; Kumar R; Monette M; Stronks HJ; Simpson AJ In-situ molecular-level elucidation of organofluorine binding sites in a whole peat soil. Environ Sci Technol 2012, 46 (19), 10508–10513. DOI: 10.1021/es3026769. [PubMed: 22946434]

(32). Martz M; Heil J; Marschner B; Stumpe B Effects of soil organic carbon (SOC) content and accessibility in subsoils on the sorption processes of the model pollutants nonylphenol (4-n-NP) and perfluorooctanoic acid (PFOA). Sci Total Environ 2019, 672, 162–173. DOI: 10.1016/j.scitotenv.2019.03.369. [PubMed: 30954815]

(33). Yan W; Qian T; Zhang L; Wang L; Zhou Y Interaction of perfluorooctanoic acid with extracellular polymeric substances - Role of protein. J Hazard Mater 2021, 401, 123381. DOI: 10.1016/j.jhazmat.2020.123381. [PubMed: 32652414]

(34). Nguyen TMH; Braunig J; Kookana RS; Kaserzon SL; Knight ER; Vo HNP; Kabiri S; Navarro DA; Grimison C; Riddell N; Higgins CP; McLaughlin MJ; Mueller JF Assessment of Mobilization Potential of Per- and Polyfluoroalkyl Substances for Soil Remediation. Environ Sci Technol 2022, 56 (14), 10030–10041. DOI: 10.1021/acs.est.2c00401. [PubMed: 35763608]

(35). Xiao F; Jin B; Golovko SA; Golovko MY; Xing B Sorption and Desorption Mechanisms of Cationic and Zwitterionic Per- and Polyfluoroalkyl Substances in Natural Soils: Thermodynamics and Hysteresis. Environ Sci Technol 2019, 53 (20), 11818–11827. DOI: 10.1021/acs.est.9b05379. [PubMed: 31553179]

(36). Brusseau ML; Rao PSC; Gillham RW Sorption nonideality during organic contaminant transport in porous media. Crit Rev Env Contr 1989, 19 (1), 33–99. DOI: 10.1080/10643388909388358.

(37). Mejia-Avendano S; Zhi Y; Yan B; Liu J Sorption of Polyfluoroalkyl Surfactants on Surface Soils: Effect of Molecular Structures, Soil Properties, and Solution Chemistry. Environ Sci Technol 2020, 54 (3), 1513–1521. DOI: 10.1021/acs.est.9b04989. [PubMed: 31922402]

(38). Nguyen TMH; Braunig J; Thompson K; Thompson J; Kabiri S; Navarro DA; Kookana RS; Grimison C; Barnes CM; Higgins CP; McLaughlin MJ; Mueller JF Influences of Chemical Properties, Soil Properties, and Solution pH on Soil-Water Partitioning Coefficients of Per- and Polyfluoroalkyl Substances (PFASs). Environ Sci Technol 2020, 54 (24), 15883–15892. DOI: 10.1021/acs.est.0c05705. [PubMed: 33249833]

(39). Wei C; Song X; Wang Q; Hu Z Sorption kinetics, isotherms and mechanisms of PFOS on soils with different physicochemical properties. Ecotoxicol Environ Saf 2017, 142, 40–50. DOI: 10.1016/j.ecoenv.2017.03.040. [PubMed: 28384502]

(40). Oliver DP; Li Y; Orr R; Nelson P; Barnes M; McLaughlin MJ; Kookana RS Sorption behaviour of per- and polyfluoroalkyl substances (PFASs) in tropical soils. Environ Pollut 2020, 258, 113726. DOI: 10.1016/j.envpol.2019.113726. [PubMed: 32006795]

(41). Jeon J; Kannan K; Lim BJ; An KG; Kim SD Effects of salinity and organic matter on the partitioning of perfluoroalkyl acid (PFAs) to clay particles. J Environ Monit 2011, 13 (6), 1803–1810. DOI: 10.1039/c0em00791a. [PubMed: 21494748]

(42). Wang M; Orr AA; Jakubowski JM; Bird KE; Casey CM; Hearon SE; Tamamis P; Phillips TD Enhanced adsorption of per- and polyfluoroalkyl substances (PFAS) by edible, nutrient-amended montmorillonite clays. Water Res 2021, 188, 116534. DOI: 10.1016/j.watres.2020.116534. [PubMed: 33125992]

(43). Yan B; Munoz G; Sauve S; Liu J Molecular mechanisms of per- and polyfluoroalkyl substances on a modified clay: a combined experimental and molecular simulation study. Water Res 2020, 184, 116166. DOI: 10.1016/j.watres.2020.116166. [PubMed: 32698092]

(44). Aly YH; Liu C; McInnis DP; Lyon BA; Hatton J; McCarty M; Arnold WA; Pennell KD; Simcik MF In Situ Remediation Method for Enhanced Sorption of Perfluoro-Alkyl Substances onto Ottawa Sand. J Environ Eng 2018, 144 (9), 04018086. DOI: 10.1061/(asce)ee.1943-7870.0001418 (acccessed 2023/01/25).

(45). Brusseau ML; Khan N; Wang Y; Yan N; Van Glubt S; Carroll KC Nonideal Transport and Extended Elution Tailing of PFOS in Soil. Environ Sci Technol 2019, 53 (18), 10654–10664. DOI: 10.1021/acs.est.9b02343. [PubMed: 31464435]

(46). Brusseau ML; Yan N; Van Glubt S; Wang Y; Chen W; Lyu Y; Dungan B; Carroll KC; Holguin FO Comprehensive retention model for PFAS transport in subsurface systems. Water Res 2019, 148, 41–50. DOI: 10.1016/j.watres.2018.10.035. [PubMed: 30343197]

(47). Gellrich V; Stahl T; Knepper TP Behavior of perfluorinated compounds in soils during leaching experiments. Chemosphere 2012, 87 (9), 1052–1056. DOI: 10.1016/j.chemosphere.2012.02.011. [PubMed: 22391048]

(48). Guelfo JL; Wunsch A; McCray J; Stults JF; Higgins CP Subsurface transport potential of perfluoroalkyl acids (PFAAs): Column experiments and modeling. J Contam Hydrol 2020, 233, 103661. DOI: 10.1016/j.jconhyd.2020.103661. [PubMed: 32535327]

(49). Lv X; Sun Y; Ji R; Gao B; Wu J; Lu Q; Jiang H Physicochemical factors controlling the retention and transport of perfluorooctanoic acid (PFOA) in saturated sand and limestone porous media. Water Res 2018, 141, 251–258. DOI: 10.1016/j.watres.2018.05.020. [PubMed: 29800833]

(50). McKenzie ER; Siegrist RL; McCray JE; Higgins CP Effects of chemical oxidants on perfluoroalkyl acid transport in one-dimensional porous media columns. Environ Sci Technol 2015, 49 (3), 1681–1689. DOI: 10.1021/es503676p. [PubMed: 25621878]

(51). Vierke L; Moller A; Klitzke S Transport of perfluoroalkyl acids in a water-saturated sediment column investigated under near-natural conditions. Environ Pollut 2014, 186, 7–13. DOI: 10.1016/j.envpol.2013.11.011. [PubMed: 24333660]

(52). Garcia RA; Chiaia-Hernandez AC; Lara-Martin PA; Loos M; Hollender J; Oetjen K; Higgins CP; Field JA Suspect Screening of Hydrocarbon Surfactants in AFFFs and AFFF-Contaminated Groundwater by High-Resolution Mass Spectrometry. Environ Sci Technol 2019, 53 (14), 8068–8077. DOI: 10.1021/acs.est.9b01895. [PubMed: 31269393]

(53). Moody CA; Field JA Perfluorinated Surfactants and the Environmental Implications of Their Use in Fire-Fighting Foams. Environmental Science & Technology 2000, 34 (18), 3864–3870. DOI: 10.1021/es991359u.

(54). Pan G; Jia C; Zhao D; You C; Chen H; Jiang G Effect of cationic and anionic surfactants on the sorption and desorption of perfluorooctane sulfonate (PFOS) on natural sediments. Environ Pollut 2009, 157 (1), 325–330. DOI: 10.1016/j.envpol.2008.06.035. [PubMed: 18722698]

(55). Johnson RL; Anschutz AJ; Smolen JM; Simcik MF; Penn RL The Adsorption of Perfluorooctane Sulfonate onto Sand, Clay, and Iron Oxide Surfaces. Journal of Chemical & Engineering Data 2007, 52 (4), 1165–1170. DOI: 10.1021/je060285g.

(56). Lee H; Mabury SA Sorption of Perfluoroalkyl Phosphonates and Perfluoroalkyl Phosphinates in Soils. Environ Sci Technol 2017, 51 (6), 3197–3205. DOI: 10.1021/acs.est.6b04395. [PubMed: 28222593]

(57). Tratnyek PG; Bylaska EJ; Weber EJ In silico environmental chemical science: properties and processes from statistical and computational modelling. Environ Sci Process Impacts 2017, 19 (3), 188–202. DOI: 10.1039/c7em00053g. [PubMed: 28262894]

(58). Sharifan H; Bagheri M; Wang D; Burken JG; Higgins CP; Liang Y; Liu J; Schaefer CE; Blotevogel J Fate and transport of per- and polyfluoroalkyl substances (PFASs) in the vadose zone. Sci Total Environ 2021, 771, 145427. DOI: 10.1016/j.scitotenv.2021.145427. [PubMed: 33736164]

(59). Team, M. P. A. R. PFAS Sites and Areas of Interest. 2022. https://www.michigan.gov/pfasresponse/investigations/sites-aoi (accessed 2022 10/18/2022).

(60). Team, M. P. A. R. Former Wurtsmith Air Force Base (Oscoda, Iosco County). 2022. https://www.michigan.gov/pfasresponse/investigations/sites-aoi/iosco-county/wurtsmith (accessed 2022 10/18/2022).

(61). Schwarzenbach RP; Gschwend PM; Imboden DM Sorption I: General Introduction and Sorption Processes Involving Organic Matter. In Environmental Organic Chemistry, 2nd ed.; John Wiley & Sons, 2002; pp 275–331.

(62). Kostarelos K; Sharma P; Christie E; Wanzek T; Field J Viscous Microemulsions of Aqueous Film-Forming Foam (AFFF) and Jet Fuel A Inhibit Infiltration and Subsurface Transport. Environmental Science & Technology Letters 2020, 8 (2), 142–147. DOI: 10.1021/acs.estlett.0c00868.

(63). Nickerson A; Maizel AC; Kulkarni PR; Adamson DT; Kornuc JJ; Higgins CP Enhanced Extraction of AFFF-Associated PFASs from Source Zone Soils. Environ Sci Technol 2020, 54 (8), 4952–4962. DOI: 10.1021/acs.est.0c00792. [PubMed: 32200626]

(64). Staff SS Rubicon Series Official Soil Description. Natural Resources Conservation Service, United States Department of Agriculture, 2012. https://soilseries.sc.egov.usda.gov/OSD_Docs/R/RUBICON.html (accessed 6/1/2019).

(65). Dwarakanath V; Kostarelos K; Pope GA; Shotts D; Wade WH Anionic surfactant remediation of soil columns contaminated by nonaqueous phase liquids. Journal of Contaminant Hydrology 1999, 38 (4), 465–488. DOI: 10.1016/s0169-7722(99)00006-6.

(66). Kostarelos K; Pope GA; Rouse BA; Shook GM A new concept: the use of neutrally-buoyant microemulsions for DNAPL remediation. Journal of Contaminant Hydrology 1998, 34 (4), 383–397. DOI: 10.1016/s0169-7722(98)00091-6.

(67). Stark JR; Cummings TR; Twenter FR Ground-water contamination at Wurtsmith Air Force Base, Michigan; Lansing, MI, 1983. http://pubs.er.usgs.gov/publication/wri834002 DOI: 10.3133/wri834002.

(68). Runkel RL Solution of the Advection-Dispersion Equation: Continuous Load of Finite Duration. J Environ Eng 1996, 122 (9), 830–832. DOI: 10.1061/(asce)0733-9372(1996)122:9(830).

(69). Li Z; Lyu X; Gao B; Xu H; Wu J; Sun Y Effects of ionic strength and cation type on the transport of per fl uorooctanoic acid (PFOA) in unsaturated sand porous media. J Hazard Mater 2021, 403, 123688. DOI: 10.1016/j.jhazmat.2020.123688. [PubMed: 33264881]

(70). Stults JF; Choi YJ; Schaefer CE; Illangasekare TH; Higgins CP Estimation of Transport Parameters of Perfluoroalkyl Acids (PFAAs) in Unsaturated Porous Media: Critical Experimental and Modeling Improvements. Environ Sci Technol 2022, 56 (12), 7963–7975. DOI: 10.1021/acs.est.2c00819. [PubMed: 35549168]

(71). Shackelford CD; Malusis MA; Majeski MJ; Stern RT Electrical Conductivity Breakthrough Curves. Journal of Geotechnical and Geoenvironmental Engineering 1999, 125 (4), 260–270. DOI: 10.1061/(asce)1090-0241(1999)125:4(260).

(72). Drummond JD; Covino TP; Aubeneau AF; Leong D; Patil S; Schumer R; Packman AI Effects of solute breakthrough curve tail truncation on residence time estimates: A synthesis of solute tracer injection studies. Journal of Geophysical Research: Biogeosciences 2012, 117 (G3), n/a-n/a. DOI: 10.1029/2012jg002019.

(73). Pedregosa F; Varoquaux G; Gramfort A; Michel V; Thirion B; Grisel O; Blondel M; Prettenhofer P; Weiss R; Dubourg V; Vanderplas J; Passos A; Cournapeau D; Brucher M; Perrot M; Duchesnay É Scikit-learn: Machine Learning in Python. J. Mach. Learn. Res 2011, 12 (null), 2825–2830.

(74). Chai T; Draxler RR Root mean square error (RMSE) or mean absolute error (MAE)? – Arguments against avoiding RMSE in the literature. Geoscientific Model Development 2014, 7 (3), 1247–1250. DOI: 10.5194/gmd-7-1247-2014.

(75). Brusseau ML Simulating PFAS transport influenced by rate-limited multi-process retention. Water Res 2020, 168, 115179. DOI: 10.1016/j.watres.2019.115179. [PubMed: 31639593]

(76). Kirby BJ Micro- and Nanoscale Fluidics: Transport in Microfluidic Devices; Cambridge University Press, 2010.

(77). Haggerty R; Gorelick SM Multiple-Rate Mass Transfer for Modeling Diffusion and Surface Reactions in Media with Pore-Scale Heterogeneity. Water Resources Research 1995, 31 (10), 2383–2400, 10.1029/95WR10583. DOI: 10.1029/95wr10583 (acccessed 2022/10/18).

(78). Shafique U; Dorn V; Paschke A; Schuurmann G Adsorption of perfluorocarboxylic acids at the silica surface. Chem Commun (Camb) 2017, 53 (3), 589–592. DOI: 10.1039/c6cc07525h. [PubMed: 27981321]

(79). Licato JJ; Foster GD; Huff TB Zeolite Composite Materials for the Simultaneous Removal of Pharmaceuticals, Personal Care Products, and Perfluorinated Alkyl Substances in Water Treatment. ACS ES&T Water 2022, 2 (6), 1046–1055. DOI: 10.1021/acsestwater.2c00024.

(80). Van den Bergh M; Krajnc A; Voorspoels S; Tavares SR; Mullens S; Beurroies I; Maurin G; Mali G; De Vos DE Highly Selective Removal of Perfluorinated Contaminants by Adsorption on All-Silica Zeolite Beta. Angew Chem Int Ed Engl 2020, 59 (33), 14086–14090. DOI: 10.1002/anie.202002953. [PubMed: 32365255]

(81). Brusseau ML The influence of molecular structure on the adsorption of PFAS to fluid-fluid interfaces: Using QSPR to predict interfacial adsorption coefficients. Water Res 2019, 152, 148–158. DOI: 10.1016/j.watres.2018.12.057. [PubMed: 30665161]

(82). Nickerson A; Rodowa AE; Adamson DT; Field JA; Kulkarni PR; Kornuc JJ; Higgins CP Spatial Trends of Anionic, Zwitterionic, and Cationic PFASs at an AFFF-Impacted Site. Environ Sci Technol 2021, 55 (1), 313–323. DOI: 10.1021/acs.est.0c04473. [PubMed: 33351591]

(83). Cowan CT; White D The Mechanism of Exchange Reactions Occuring Between Sodium Montmorillonite and Various n-Primary Aliphatic Amine Salts. Transactions of the Faraday Society 1958, 54, 691–697.

(84). Kögel-Knabner I 13C and 15N NMR spectroscopy as a tool in soil organic matter studies. Geoderma 1997, 80 (3–4), 243–270. DOI: 10.1016/s0016-7061(97)00055-4.

(85). Oades JM; Gillman GP; Uehara G Interactions of Soil Organic Matter and Variable-Charge Clays. In Dynamics of soil organic matter in tropical ecosystems, Oades JM, Uehara G Eds.; University of Hawaii, 1989; pp 69–95.

(86). Parker BA; Knappe DRU; Titaley IA; Wanzek TA; Field JA Tools for Understanding and Predicting the Affinity of Per- and Polyfluoroalkyl Substances for Anion-Exchange Sorbents. Environ Sci Technol 2022, 56 (22), 15470–15477. DOI: 10.1021/acs.est.1c08345. [PubMed: 36265138]

(87). Halgren TA Merck molecular force field. I. Basis, form, scope, parameterization, and performance of MMFF94. Journal of Computational Chemistry 1996, 17 (5–6), 490–519. DOI: 10.1002/(sici)1096-987x(199604)17:5/6<490::Aid-jcc1>3.0.Co;2-p.

(88). Hanwell MD; Curtis DE; Lonie DC; Vandermeersch T; Zurek E; Hutchison GR Avogadro: an advanced semantic chemical editor, visualization, and analysis platform. J Cheminform 2012, 4 (1), 17. DOI: 10.1186/1758-2946-4-17. [PubMed: 22889332]

(89). Li W; Hu Y; Bischel HN In-Vitro and In-Silico Assessment of Per- and Polyfluoroalkyl Substances (PFAS) in Aqueous Film-Forming Foam (AFFF) Binding to Human Serum Albumin. Toxics 2021, 9 (3), 2305–6304. DOI: 10.3390/toxics9030063.

(90). Park M; Daniels KD; Wu S; Ziska AD; Snyder SA Magnetic ion-exchange (MIEX) resin for perfluorinated alkylsubstance (PFAS) removal in groundwater: Roles of atomic charges for adsorption. Water Res 2020, 181, 115897. DOI: 10.1016/j.watres.2020.115897. [PubMed: 32450335]

(91). Liu Y; Qi F; Fang C; Naidu R; Duan L; Dharmarajan R; Annamalai P The effects of soil properties and co-contaminants on sorption of perfluorooctane sulfonate (PFOS) in contrasting soils. Environmental Technology & Innovation 2020, 19. DOI: 10.1016/j.eti.2020.100965.

(92). Ayawei N; Ebelegi AN; Wankasi D Modelling and Interpretation of Adsorption Isotherms. Journal of Chemistry 2017, 2017, 3039817. DOI: 10.1155/2017/3039817.

(93). Schaefer CE; Nguyen D; Christie E; Shea S; Higgins CP; Field JA Desorption of Poly- and Perfluoroalkyl Substances from Soil Historically Impacted with Aqueous Film-Forming Foam. J Environ Eng 2021, 147 (2), 06020006. DOI: 10.1061/(asce)ee.1943-7870.0001846 (acccessed 2023/01/25).

(94). Fabregat-Palau J; Vidal M; Rigol A Modelling the sorption behaviour of perfluoroalkyl carboxylates and perfluoroalkane sulfonates in soils. Sci Total Environ 2021, 801, 149343. DOI: 10.1016/j.scitotenv.2021.149343. [PubMed: 34418616]

SYNOPSIS

Interactions between 34 PFAS and organic and the soil matrix were examined in column experiments to derive a predictive algorithm for the retention of anionic and zwitterionic PFAS in AFFF affected soil.

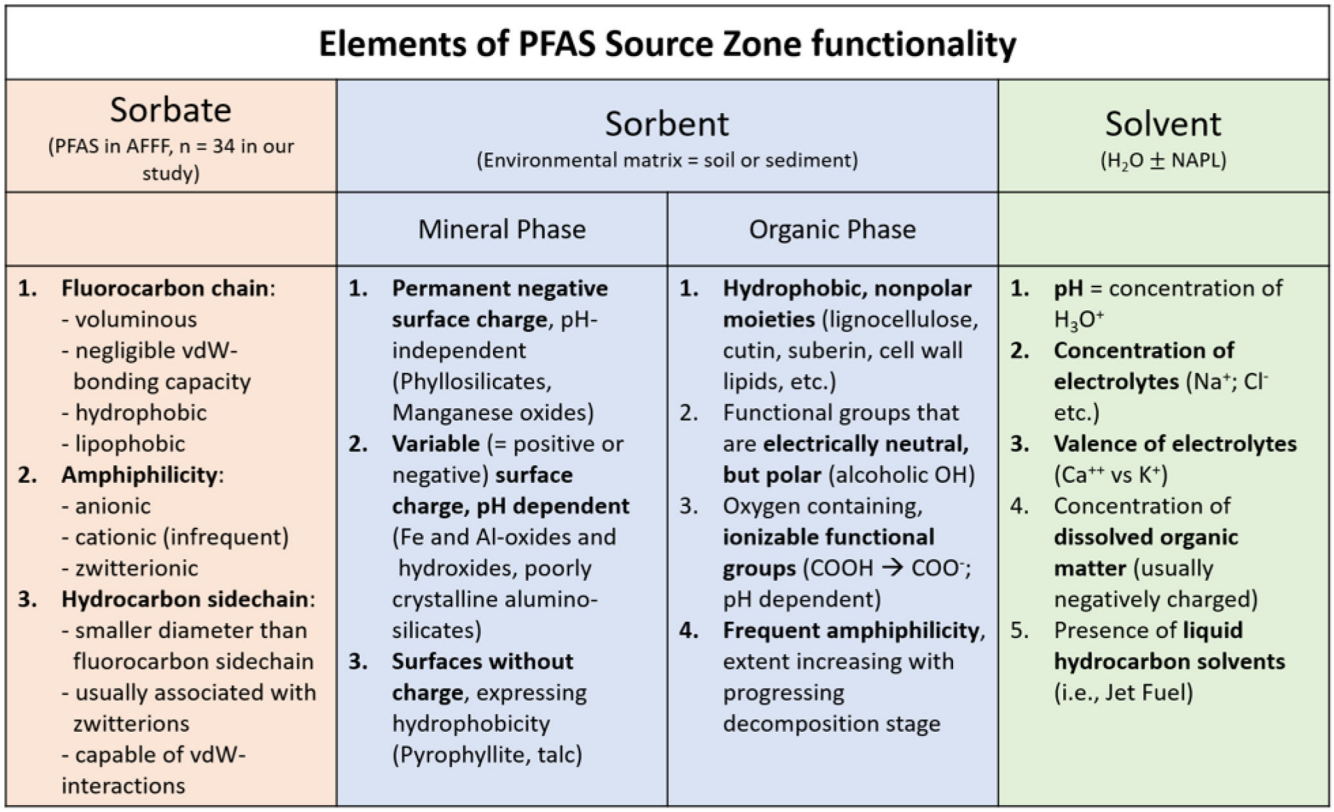

Figure 1:

Summary of the system properties that are potentially involved in determining the retention of the complex PFAS mixtures found in AFFF. Source zone: the portion of a site that contributes contaminant mass to the ground water plume. vdW = van der Waals forces; NAPL = non aqueous phase liquid.

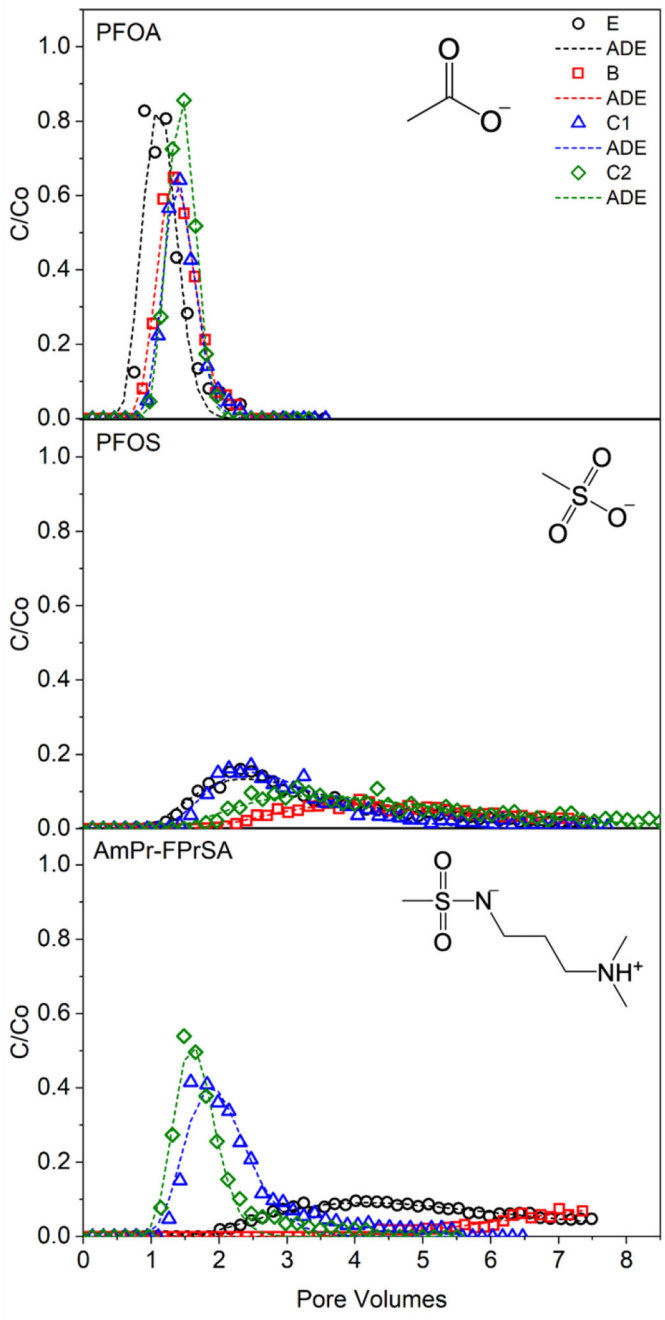

Figure 2.

Breakthrough curves for three PFAS from all soil columns. C/Co (y-axis) for measured values (open points) and predicted values using an equilibrium advection-dispersion fit (dashed line) are shown for PFOA (top), PFOS (middle), and AmPr-FPrSA (bottom). Breakthrough is plotted as a function of pore volumes (x-axis). Initial concentrations of applied PFAS are in Table S5. Abbreviated structures with functional head groups only are shown for each PFAS.

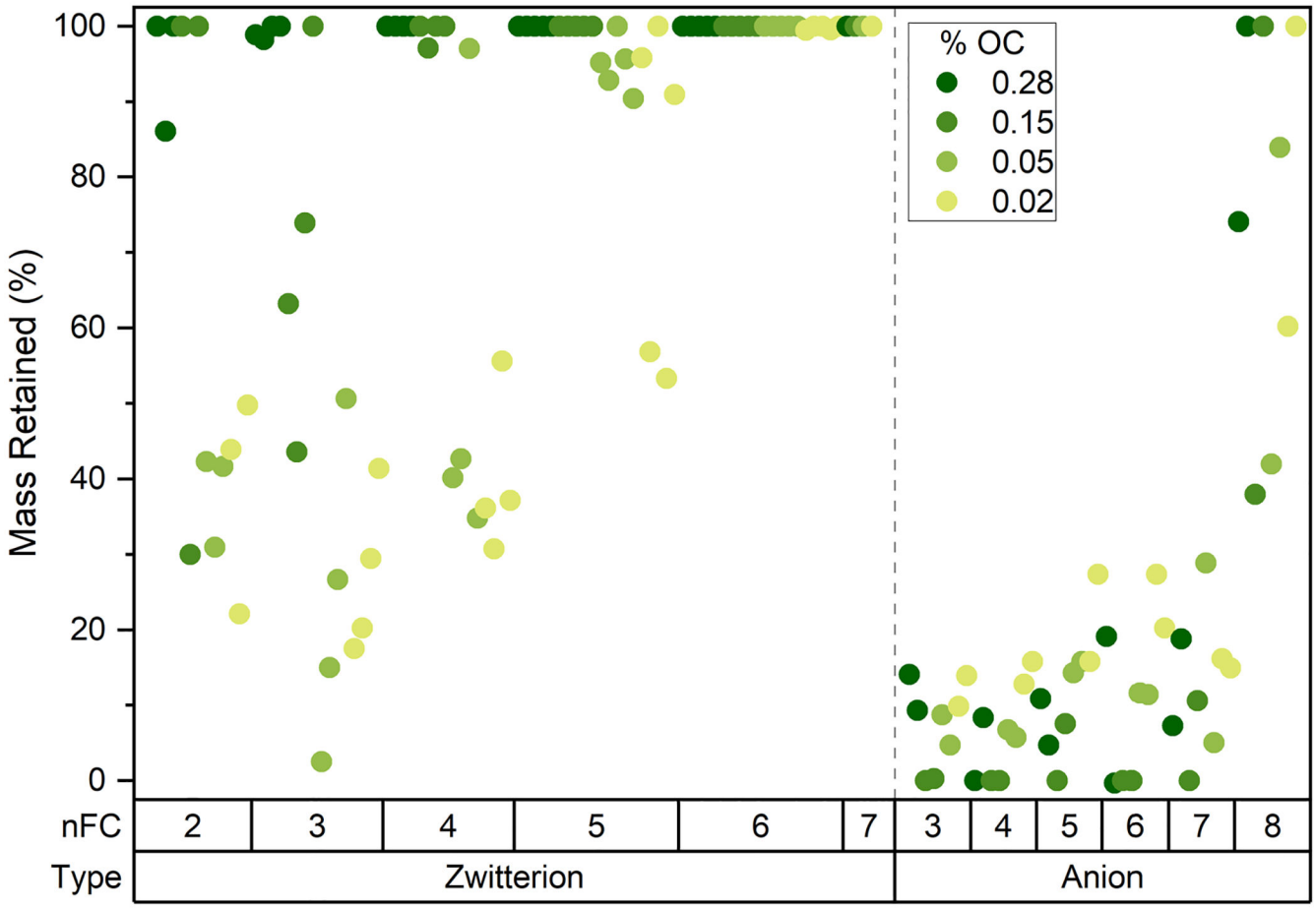

Figure 3.

Mass retained for all PFAS (n = 34) and soil (% OC) combinations (n = 4) (N = 136 observations in total) organized by zwitterions (left) and anions (right) and number of fluorinated carbons (nFC) (x-axis). Intensity of green color corresponds with OC concentrations (0.28% to 0.02%). Mass Retained data were determined after flushing with five pore volumes of synthetic tap water.

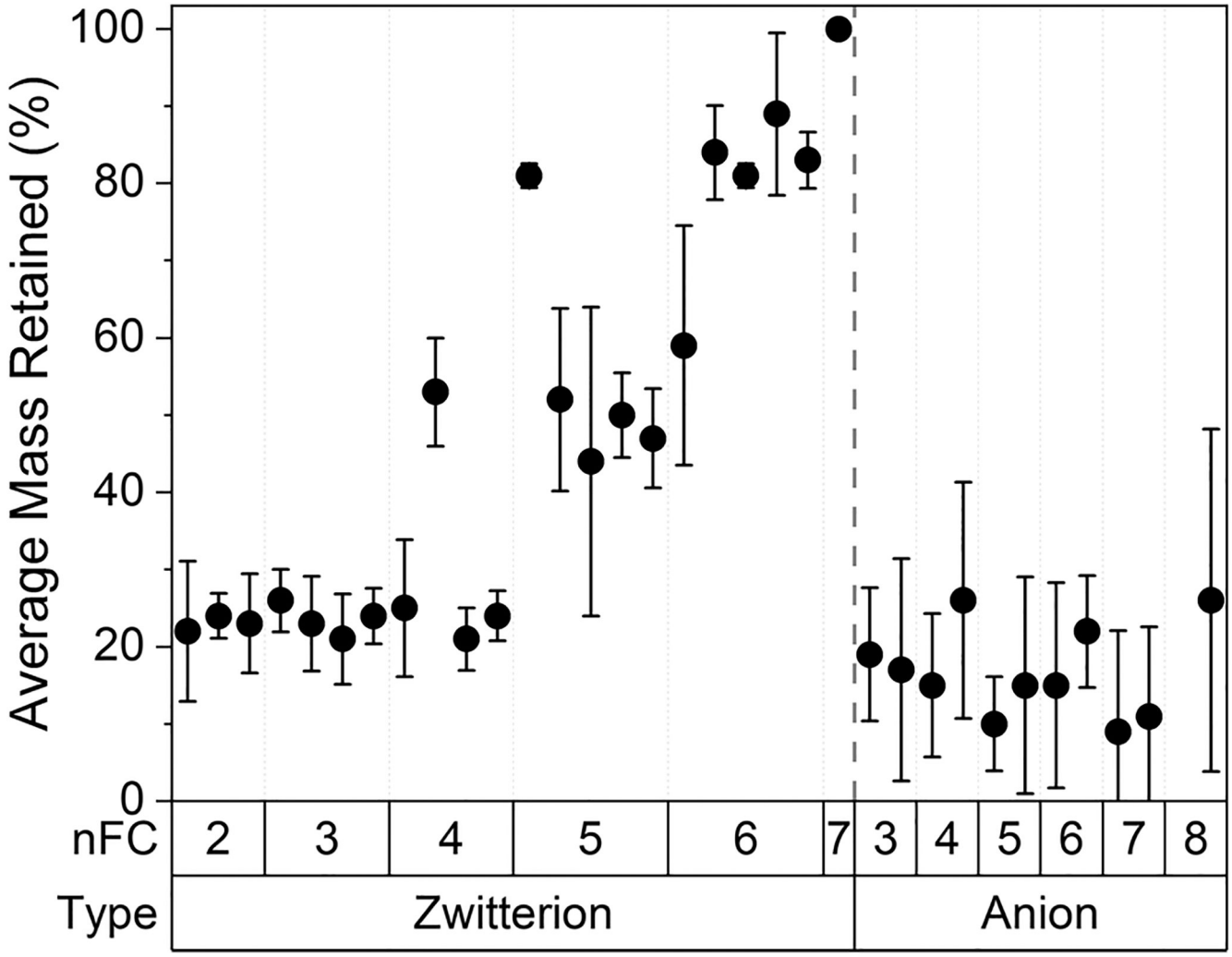

Figure 4.

Average (n=3) PFAS mass retained in Accusand (no OC) organized by zwitterions (left) and anions (right) and number of fluorinated carbons (nFC) (x-axis). The dimensions of the scale for the x-axis category nFC are proportional to the number of PFAS species in each group (larger spacing = more PFAS species and vice versa). Error bars are one standard deviation. Mass Retained data were determined after flushing with five pore volumes of synthetic tap water.

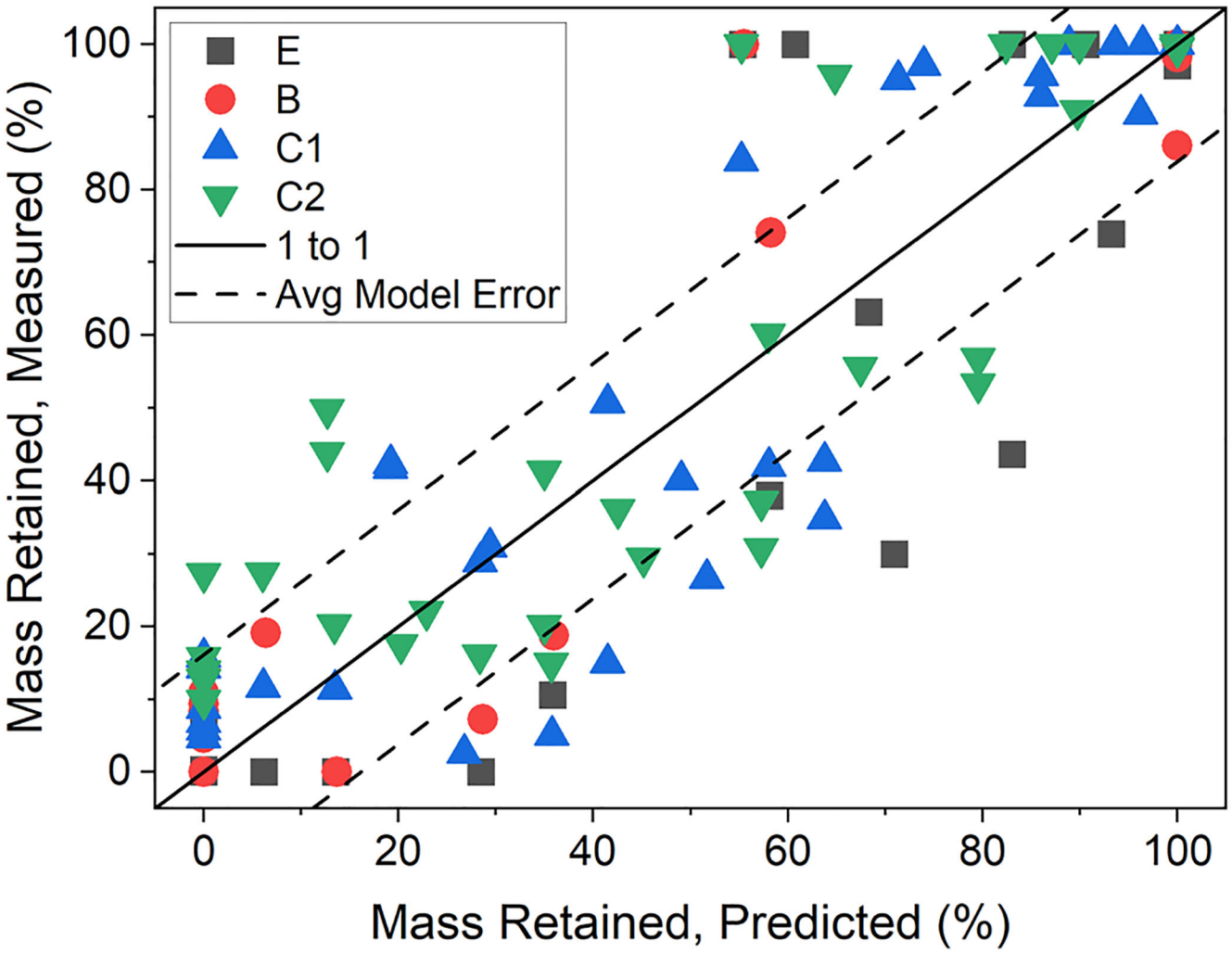

Figure 5.

Experimentally measured M_R plotted as a function of model predicted M_R. Solid line represents M_R predicted = M_R measured, dashed lines indicate average error.